Journal of Applied Electrochemistry (2024) 54:731–738
https://doi.org/10.1007/s10800-023-02007-6

RESEARCH ARTICLE

A quantitative and qualitative study of gas generation observed in $LiFePO_4$–$TiNb_2O_7$ cells

Benjamin Mercier-Guyon[1] · Jean-François Colin[1] · Irina Profatilova[1] · Sébastien Martinet[1]

Received: 16 May 2023 / Accepted: 15 October 2023 / Published online: 30 November 2023

Abstract

Since 20 years, titanium oxide materials and in particular, lithium titanate spinel $Li_4Ti_5O_{12}$ (LTO) were considered as promising negative electrode materials for lithium-ion cells. In the case of the $TiNb_2O_7$ compound (TNO), which has a larger theoretical lithiation capacity of 388 mAh g^{-1}, few studies have focused on the outgassing of the material. In this work, we quantified the volume produced as a function of different cycling parameters and then characterized the produced species and show a prevalence of H_2 gas. The use of carbon coating as a mitigation strategy and its limitation is also discussed.

Graphical abstract

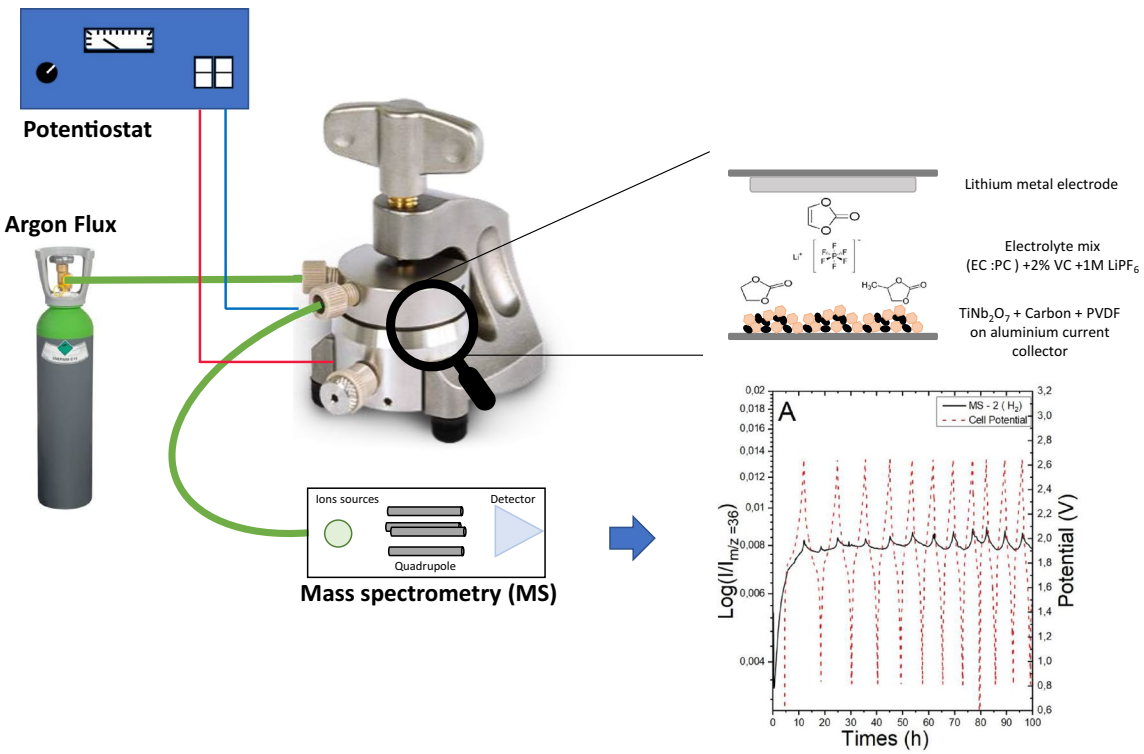

Keywords $TiNb_2O_7$ · $Li_4Ti_5O_{12}$ · Gassing · *Operando* analysis

✉ Jean-François Colin
jean-francois.colin@cea.fr

[1] Univ. Grenoble Alpes, CEA, LITEN, 38054, Grenoble, France

1 Introduction

Rechargeable lithium-ion batteries (LiBs) have been widely used as power sources for various applications, including portable electronic devices, electrical vehicles and large-scale energy storage [24].

Quickly becoming the most used technology, LiBs cells mainly use graphite as negative electrode material because of its low cost and good theoretical capacity (372 mAh g^{-1}) [4]. However, this electrode suffer from stability issues, such as thermal runaway [19, 20] that is usually the final consequence of uncontrolled SEI growth, lithium plating, and dendrite formation after cycling in hard conditions.

Alternatively negative electrodes using titanates such as lithium titanate spinel $Li_4Ti_5O_{12}$ (LTO) have been extensively studied. Its high operating voltage preventing lithium plating as well as its long cycle life (> 20 000 cycles) and its ultra-low volume change during the lithium insertion [7] made this technology a good solution to substitute graphite electrode. However, a low specific capacity (175 mAh g^{-1}) [28] as well as a gassing phenomenon drastically hinder the deployment of this material [3].

With this drawback in mind, Goodenough et al. showed in 2011 that $TiNb_2O_7$ (TNO) can be used as a negative electrode material [11], keeping LTO's advantages (e.g., high power ability, long life, and ultra-safe performance in abusive conditions) but offering a higher theoretical capacity of 388 mAh g^{-1}. This value is almost twice the one of LTO due to five exchangeable electrons (Ti^{4+}/Ti^{3+}, Nb^{5+}/Nb^{3+}) and comparable to the one of graphite [6].

Widely studied for LTO [12, 14, 16], titanates materials are well known for their gassing behavior. However, only few studies have been carried out on this specific point for TNO [5, 21].

Buannic et al. [5] highlighted a strong dependence of generated gases volume to the specific surface of the active material. They have also reported that gassing phenomenon could be more intense in TNO cells than in LTO's ones, pointing out the presence of niobium cation at the surface of the material.

More recently, Parikh et al. [21] reported the first *operando* gas analysis on TNO-NMC cell, confirming the hypothesis that the gas generated is the result of the decomposition of the solvent in the electrolyte during the formation of a pseudo-SEI on the surface of the active material grains. The formation of SEI has also been observed using various characterization techniques [X-ray photoelectron spectroscopy (XPS), Fourier transform infrared (FTIR), scanning electron microscopy (SEM), and high-resolution transmission electron microscopy (HRTEM)] by Wu et al. [27]. They also show that using a carbon coating could lead to a drastic reduction of the generated volume.

In this study, we chose to characterize the volume of gas produced by the technique of Archimedes weighing on pouch cell as well as the chemical species produced during cycling by online electrochemical mass spectrometry *operando*.

2 Methods

2.1 Material synthesis

The mixed oxide $TiNb_2O_7$ was prepared via a simple one-step solid-state synthesis.

Titanium oxide (TiO_2 anatase, 99.0%, Huntsman) and niobium pentoxide (Nb_2O_5, 99.9%, Aldrich) powders have been used as precursors and introduced in stoichiometric amounts. The mix was ball milled (PM 100 CM, Retsch) 4 h at 400 rpm using agate bowl and balls. Finally, the product was calcined at 1100 °C, for 16 h in a muffle furnace under air.

The coated material was obtained by mixing polyvinyl alcohol (PVA, Solvay), used as a carbonaceous precursor, with TNO in a mortar and then decomposing the mixture in a tubular furnace under inert atmosphere (Argon) at 800 °C for 8 h. Final product has been characterized in TGA under air and its carbon content evaluated to 0.85 wt%.

After cooling, the powder was crushed manually with a mortar and pestle to reduce its granulometry. To ensure the purity of the synthesized phase, X-ray powder diffraction (XRD) was carried out on a Brüker D8 Advance using a Cu anticathode. This reveals a pure $TiNb_2O_7$ material as shown in Fig 1.

The particle size distribution (PSD) was obtained on a Malvern Mastersizer MS-S.

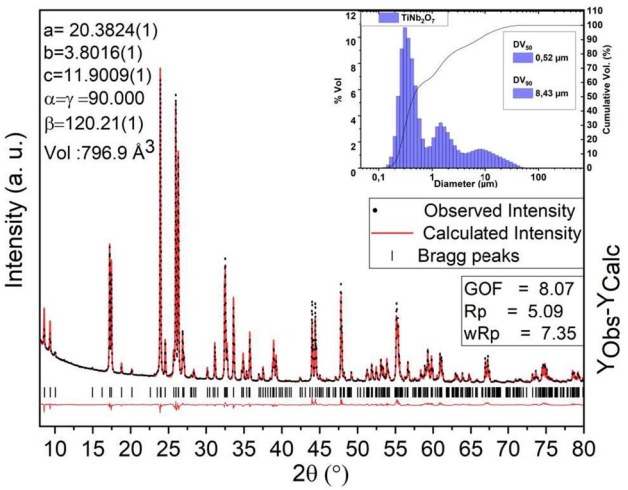

Fig. 1 XRD and PSD of the active material

2.2 Electrochemical characterization

Electrodes are made from an organic formulation. Firstly, our active material was mixed with an electronic conductor (Super P C65 from Imeris) in cyclohexane. After total evaporation of the latter, the binder was added with a solution of PVDF Solef 1530 (Arkema) at 10 wt% in *N*-methyl-2-pyrrolidone (NMP, Sigma Aldrich) until a formulation of 80% active material, 10% electronic conductor 10% binder, and a dry extract of 30% was reached.

The slurries were then coated onto an aluminum foil. Two different coating processes were used. Lab-scale electrode was produced using a laboratory coating table (Elcometer 4330) and pilot-scale electrode was produced on an Upscale Coating Machine built by Ingecal.

Both kinds of electrodes were then calendered and dried. Their typical loading is 1.8 mg cm^{-2} corresponding to a theoretical surface capacity of 0.7 mAh cm^{-2}. With a density of 1.35, the electrodes have a porosity of 60% after calendering.

To allow a comparison of the gassing of the two materials, $Li_4Ti_5O_{12}$ electrodes were made in the same way from active materials supplied by PRAYON.

For electrochemical measurements, we used a full cell set-up. Counter electrodes were made following the same process, using $LiFePO_4$ (LFP further), industrial grade supplied by PRAYON, displaying a loading of 0.82 mAh cm^{-2} and achieving a balancing of 120% vs. negative electrodes ensuring full use of the negative electrode. We choose this compound rather than a NMC material type because of its great stability and its flat voltage plateau.

Pouch cells were assembled under controlled atmosphere (− 20 °C dew point), by stacking 2 single-side-coated TNO electrodes (3.5 × 3.5 cm, 24.5 cm^2) and a double-side-coated LFP electrode (3.75 × 3.75, 28.2 cm^2), each side separated by a polypropylene separator (CG2500, Celgard). 800 µL of a solution of ethylene carbonate (EC), propylene carbonate (PC), dimethyl carbonate (DMC) (1:1:3 vol), and Lithium hexafluorophosphate $LiPF_6$ (1 M) (LP100, UBE Industries) were used to activate the cell.

2.3 Gases studies

2.3.1 Qualitative studies

Operando gas analysis required the use of specially designed cells, ECC-Air cell provided by El-Cell®, allowing argon circulation. Circular single-side electrodes of LFP and TNO with a diameter of 16 mm were assembled with polypropylene separator (CG2500, Celgard) in an Argon-filled glovebox ($[H_2O]$ and $[O_2]$ < 0.1 ppm) and activated with 150 µL of EC, PC (1:1) with 2% vinylene carbonate (VC) and Lithium hexafluorophosphate $LiPF_6$ (1 M) (UBE Industries). This electrolyte is less volatile due to the absence of DMC and limits the risk of saturation of the mass spectrometer sensor. Pure argon flow of 2.2 mL min^{-1} was used through the El cell to push the gases formed during the electrochemical reactions to a mass spectrometer. Pfeiffer Omnistar GSD320 mass spectrometer was used for the gas analysis.

Galvanostatic discharges and charges were performed on a Bio-logic VMP laboratory battery tester at C/10 rate (assuming C = 388 mAh g^{-1}) in a potential range within 2.6–0.8 V vs. Li^+/Li.

2.3.2 Quantitative studies

The measurement of the produced gas volumes, either following a calendar aging or during cycling, was carried out using the Archimedes density method. Initially introduced by Aiken et al. [1], this technique is based on Archimedes' principle 1.

$$F_{\text{Archimedes}} = \rho V g \tag{1}$$

with $F_{\text{Archimedes}}$ is the Archimedes' principle, ρ is the fluid density, V is the submerged volume in m^3, and g is the acceleration of gravity in m s^{-2},

Pouch cells were weighed with a precision scale, in air and immersed in an ethanol solution. The apparent weight P_{App} can be written as in the relation 2:

$$P_{\text{App}} = P_{\text{Real}} - F_{\text{Archimedes}} \tag{2}$$

with P_{App} the apparent weight and P_{Real} obtained from the mass.

Archimedes' principle can be described with the following relation 3:

$$F_{\text{Archimedes}} = P_{\text{Fluid}} = \rho_{\text{Fluid}} \cdot V_{\text{Fluid}} \tag{3}$$

with P_{Fluid}, the weight of displaced liquid, ρ_{Fluid} the fluid density, and V_{Fluid} the fluid volume.

By defining ΔP as $\Delta P = P_{\text{Real}} - P_{\text{App}}$, we obtain the relation 4 allowing to know the volume of the cell V_{Cell}:

$$V_{\text{Cell}} = V_{\text{Fluid}} = \frac{\Delta P}{\rho_{\text{Fluid}}}. \tag{4}$$

The measurement of the temperature of the fluid, in our case absolute ethanol (CARLO ERBA Reagents), makes it possible to determine its exact density via the relation 5 [8].

$$\rho_{\text{EtOH}} = -8.461834 \times 10^{-4} \times T + 0.8063372. \tag{5}$$

Measurements have been carried out either after periods of calendar storage of the cells at room temperature (22 °C) or after cycling. In all cases, for each considered series of samples, the same cell was weighed and the plotted volume mean the measured volume of gas at the time mentioned (number of cycles or storage time).

For relative comparison, even if the electrode loadings were designed to be nearly the same, every measured gases volume was normalized by the negative (either TNO or LTO) active material mass.

3 Results and discussion

3.1 Volume of gas produced in LFP/TNO cells

Figure 2 displays both discharge capacity and gas volume produced during cycling in different setups. It can be noted that, despite a doubled specific discharge capacity compared to the LTO cell, the TNOs based cells also generated almost twice the gas volume, regardless of the electrode processing method used. For lab-scale electrodes, the gas volume produced upon cycling is almost three times higher than for the LTO electrode.

It seems that the physicochemical reaction, leading to the gas formation does not follow the same reaction path: in case of LTO, we note a very quick stabilization of the produced volume, without any evolution after 10 cycles, whereas for both TNO cases, the gas seems to be continuously evolved during the whole experiment.

We can suppose that the passivation layer formed on the surface of the electrodes is not stable and fractures at each cycle, following the important expansion of the particles observed in in situ X-ray diffraction [10], leading to a constant gas formation [2].

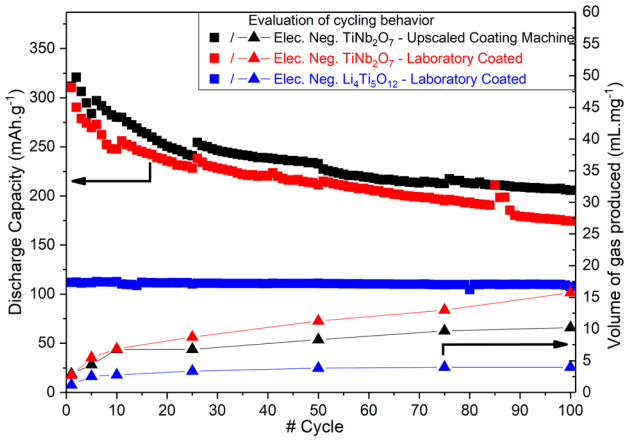

Fig. 2 Comparison of the volume of produced gas (triangle, right scale) and electrochemical performances (square, left scale) for the TNO according to the type of coating ($TiNb_2O_7$- Upscale Coating Machine, Black series and Laboratory Coated, Red series) and the LTO ($Li_4Ti_5O_{12}$ Laboratory Coated, Blue series). The small jumps in capacity observed around 25, 50, and 85 cycles are linked to isolated trouble of thermal regulation in the cycling chamber. (Color figure online)

We have also noticed that the coating method used to produce the electrodes plays a very important role for the electrochemical performances as well as for the gas production during cycling. Both TNO electrodes were designed to have similar characteristics (loading, porosity, etc.) but the use of pilot-scale coating bench leads to a better homogeneity allowing a more efficient percolation for the electronic network. In consequence, we can notice a better electrochemical performance as well as a higher mechanical resistance of the electrode during cycling, which probably leads to an improved accommodation of the volume expansion of the material and limits the constant reformation of the passivation layer.

Following these observations, we also considered the use of a carbon coating on the material to improve its electrochemical behavior and try to reduce the gassing phenomenon. This solution have been widely studied for different kinds of active materials in lithium-ion battery field [15] and in the LTO case in particular by He et al., showing a higher stability of the passivation layer and a lower gassing production inside the cell [13].

Figure 3 shows the result obtained for both carbon-coated and raw TNO. Carbon-coated material has been synthesized while targeting a final formulation with 0.8 wt% of C. This formulation had previously demonstrated interesting performance in rigid casing.

It can be noticed that the insertion capacity is initially much higher than the one of the uncoated $TiNb_2O_7$ material. However, this trend is reversed after 40 cycles when the insertion capacities of the coated sample fell below those of the untreated compound. In terms of gas volume, the $TiNb_2O_7$/C composite produces about 10% less gas, which proves a positive effect of the treatment.

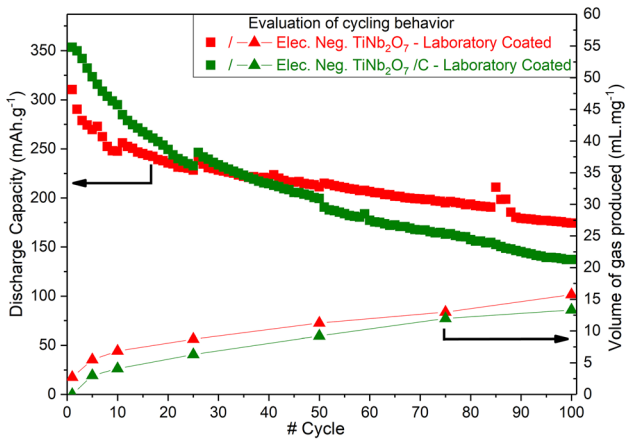

Fig. 3 Comparison of the volumes of gas produced (triangle, right scale) and electrochemical performances (square, left scale) for two TNO negative electrodes: the raw material ($TiNb_2O_7$, Red series) and the carbon-coated material ($TiNb_2O_7$/C, green series). (Color figure online)

It seems that the carbon coating limits the formation of gas during cycling. It is possible that coating the TNO particles with a thin layer of carbon creates an interface between the surface of the active material and the electrolyte, thus preventing/limiting the decomposition of the electrolyte on the surface of the TNO grains.

However, by improving the insertion capacities on the first slow cycles through an optimization of the contacts between the active particles and the network of carbonaceous electronic conductors, it is likely that the internal degradation of the material is also accelerated.

If we consider the volume of gas generated during the storage at room temperature, i.e., without imposed electrochemical activity for two identical material samples, as it is shown in Fig. 4, the carbon coating leads to a 60% gas volume reduction compared to the untreated compound.

It can also be noted that, for both measured samples, the production of gas seems to take place almost immediately. The volume of gas produced hardly changes after 7 days and the maximum value is reached after 14 days, showing an internal electrochemical process, leading to the formation of passivation layer onto the grains, mainly composed of a degraded electrolyte [2].

The comparison between the amounts of gas formed with and without cycling as a function of a duration of the measurements brings new elements to the discussion. It appears that the volume of gas generated in the case of calendar storage reaches its maximum value more quickly before staying a plateau, generating even more gas during the first 7 days than in the case of cycling, whatever the studied material is. This fact supports our hypothesis that a contact of TNO with the electrolyte generates an interfacial layer resulting from the electrolyte degradation and this process forms a certain volume of gas. However, in the case of cycling, the significant evolution of the particle size will lead to a continuous regeneration of this layer and consequently of the gas.

Therefore, the carbon coating appears to be a limited solution. The electrode formulation and the carbon coating ratio still could be optimized; however, most probably cannot solve all the problems.

Another critical point could be the quality of the used electrolyte and more specifically, the water content. The impact of high hydration on TNOs cycling performance and gas production was qualified. Thus, we examined the electrochemical performances and volume of gas produced by two cells, where one was activated with a 300 ppm hydrated electrolyte and the other one with a standard electrolyte. The results are reported in Fig. 5.

As expected, the cell containing 300 ppm of H_2O shows a significant loss of capacity compared to its non-hydrated counterpart. Similarly, gas generation is strongly impacted by the addition of water. The volume of gas produced in the case of the hydrated electrolyte increases by almost 30%. Indeed, it is commonly accepted that an excessive level of water in the system, which may be due to poor electrode drying or hydrated electrolyte, could lead to a generation of a large volume of gas through an electrolysis mechanisms at the surface of the electrodes [18].

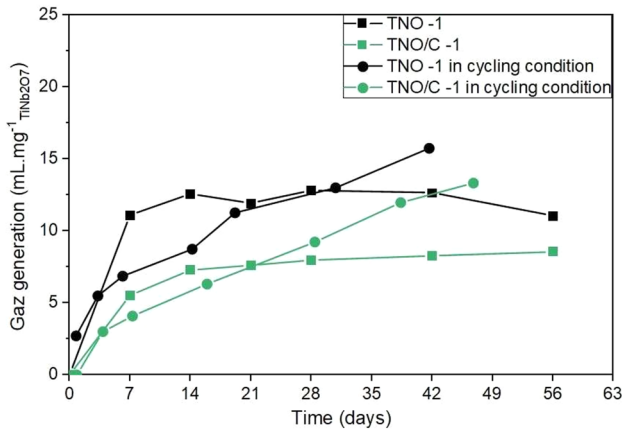

Fig. 4 Gas production versus times of calendar stored cells for two different negative lab-coated electrodes: $TiNb_2O_7$ (TNO, black solid square series) and $TiNb_2O_7$ carbon-coated (TNO/C, green solid square series). For comparison, the volume of gas generated during cycling (C/10) as a function of time has also been added: $TiNb_2O_7$ (TNO, black solid circle series) and $TiNb_2O_7$ carbon-coated (TNO/C, green solid circle series). (Color figure online)

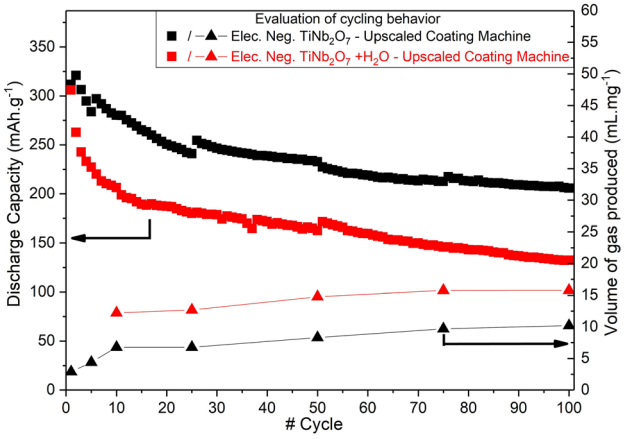

Fig. 5 Influence of electrolyte water content on the electrochemical performance and gassing behavior of LFP/TNO cells: Comparison of the volume of gas produced (triangle, right scale) and electrochemical performances (square, left scale) for the two electrolyte "grades": the battery grade ($[H_2O] < 20$ ppm) ($TiNb_2O_7$, Black series) and the hydrated electrolyte ($[H_2O] = 300$ ppm) ($TiNb_2O_7 + H_2O$, Red series)

3.2 Analysis of produced gaseous chemical species during cycling

To identify the gases formed during cycling, the use of online electrochemical mass spectrometry was necessary. This technique allows detection and identification of gases evolved by measuring their mass-to-charge ratios (*m/z*). Six different signals were monitored *operando* during the electrochemical test: $m/z = 2$ for H_2, $m/z = 26$ for C_2H_4, $m/z = 18$ for H_2O, $m/z = 28$ for CO, $m/z = 41$ for C_3H_6, and $m/z = 44$ for CO_2.

A $TiNb_2O_7$-based electrode was assembled facing a $LiFePO_4$ counter electrode in an ECC-Air cell. LFP-based counter electrode is beneficial for this kind of measurements due to the fact that does not generate gas during cycling [22]. Therefore, the gas observed during this experiment originates only from the TNO-based electrode. The electrolyte had to be adapted using a mixture of EC:PC (1:1) + 2% VC, 1 M $LiPF_6$ to reduce its vapor pressure and to avoid penetration of organic carbonate solvents vapors to the mass spectrometer. Cycling at C/10 was carried out over 11 cycles using a potentiostat. The results are shown in Fig. 6.

Plotting the cell voltage together with corresponding mass spectrometry signals allowed identifying the potential windows and onset voltages for the gas formation. Considering the cycles 1 and 2, it can be seen from the curve A in Fig. 6 reflecting the formation of H_2 that the generation of gas takes place at the end of the charges with an onset voltage of around 2.0 V and a peak corresponding to the end of charge. In addition, there is minor H_2 contribution at the end of discharges. Remarkable gas formation peaks were also detected for C_2H_4, C_3H_6, CO, and CO_2 during the first cycles at the end of charges where the potential of a lithiated TNO electrode is the lowest. These observations are in line with our hypothesis suggesting a formation of an interfacial layer on the surface of TNO-based electrode in contact with the electrolyte. It is known that the electrochemical reduction of EC mostly leads to formation of C_2H_4, while a reductive decomposition of PC leads to C_3H_6. VC can be responsible for a CO_2 production at low potentials [23].

Looking at overall trends for formation of gases during 11 cycles, hydrogen seems to be the predominant gas produced constantly during the electrochemical test. It seems to be a very similar case to LTO-containing LIBs where continuous H_2 evolution was detected [25, 26]. Up to now, there

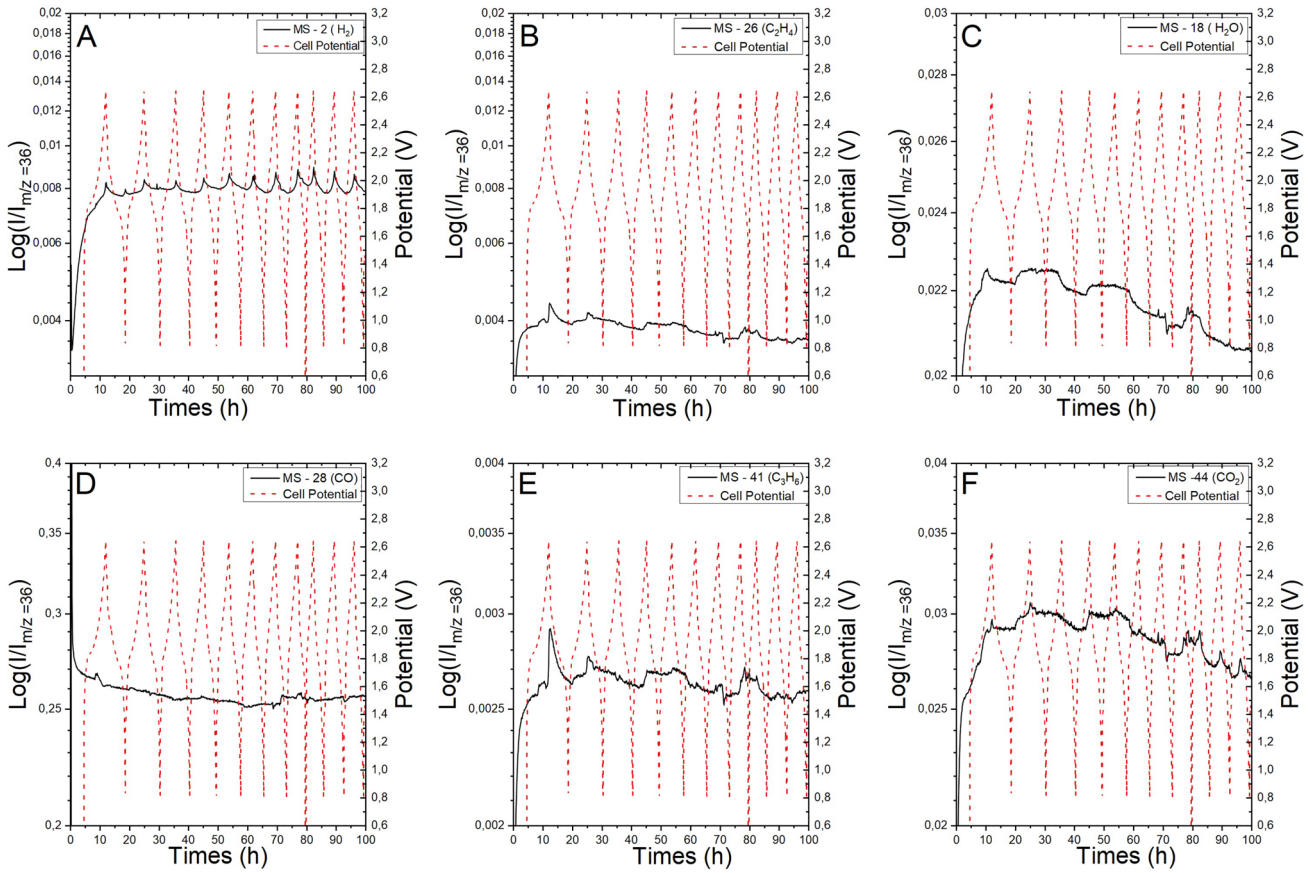

Fig. 6 Gases production measurements by *operando* mass spectrometry **A** H_2, **B** C_2H_4, **C** H_2O, **D** CO, **E** C_3H_6, and **F** CO_2

is no consensus in literature concerning a precise mechanism for H_2 formation during cycling/storage of LTO-based cells. Among the main possible ways are H_2 formation via reactions of traces of moisture and HF, spontaneous solvent decomposition on LTO surface giving protic species, the self-charge of the lithiated-LTO electrodes mediated by water [9, 29]. It is likely that the main sources of gassing in LTO are reactions between the electrolyte and the electrode surface with complicated multi-step mechanism [14].

The investigation of precise mechanism for TNO degassing was not within the scope of the present work and it requires systematic further study taking into account a complexity of the problem as seen from a similar LTO case. It should be pointed out that the electrodes and all cell components were dried properly before conducting electrochemical tests and highly pure Ar was used as a carrier gas for the OEMS investigation. Therefore, the trace amount of water initially present in the cell could not be responsible for a continuous H_2 evolution during 11 cycles. Several C_2H_4 and CO_2 peaks can be observed after the first two cycles at the end of charges; however, due to their lower intensity they are not easily detectable. We suggest that, by analogy with LTO, a degassing of a TNO-based electrodes is mostly due to the reactivity of electrolyte components (solvents and salts) with surface of the active material (the polymerization of the solvents of the electrolyte or the degradation of the lithium salts [17]) with minor contribution from electrochemical reduction of traces of water.

4 Conclusion

To conclude, a quantification and analysis of gases produced by Li-ion cells during cycling have been conducted using cells with $TiNb_2O_7$ negative electrodes and $LiFePO_4$ positive electrodes.

The measurement of gas volumes following calendar storage tends to show that once the passivation layer is formed, the gas release seems to be very strongly reduced.

On the other hand, the cycling leads to a continuous increase of the gas volume for the cell. Thus, we can propose that a strong volume variation for the active material particles during lithiation and delithiation leads to a continuously fractured/reformed interfacial layer accompanied by a quasi-continuous degassing.

This hypothesis is corroborated by the difference in results obtained for the laboratory-made electrodes of poorer quality and for the pilot-scale ones. A better dispersion and a stronger carbonaceous network allowed a better accommodation of the volume variation for the material and thus probably significantly reduced the volume of gas produced during cycling.

Considering the *operando* gas measurements, the obtained results are quite similar to those obtained by Parikh et al. [21] despite of using different counter electrodes and operating conditions. However, the authors were not able to detect H_2 during the *operando* gas measurements due to technical reasons. Using a well-known stable and non-degassing active material, such as LFP, we managed to demonstrate that the volume of gas produced by the TNO prevail over the other reactions which could take place on the positive electrode in the case of a full cell. Moreover, the chemical composition of produced gases seems to be linked to the used electrolyte components, leading to H_2, CO_2, and C_nH_{2n+2} formation mostly at the end of charges. The dominant gas is H_2, which is evolved continuously during cycling, similar to LTO-based electrodes.

Different strategies to improve the behavior and performance of $TiNb_2O_7$ electrodes have been also explored. The addition of a carbon coating by thermal decomposition of polymer precursor on the surface of the grains of active material lead to formation of a protective and conductive interface between the electrode and the electrolyte. This layer partially inhibited the mechanisms of the electrolyte decomposition catalyzed by the presence of Ti^{4+} on the surface of the grains.

The improvement of the conditions of realization of these coatings (process, reagents, final carbon rate, etc.) could lead to a better bonding of this layers with grains. This could be a promising way for a future large-scale marketing of the material.

Acknowledgements The authors acknowledge CEA-INSTN for Ph.D. funding awarded to Benjamin Mercier-Guyon. This project has received funding from the European Union's Horizon 2020 research and innovation program under Grant Agreement No. 875126 (CoFBAT).

Author contributions BM-G wrote the main manuscript text and prepared figures.All authors reviewed the manuscript.

Declarations

Conflict of interest The authors declare no competing interests.

References

1. Aiken CP, Xia J, Wang DY et al (2014) An apparatus for the study of in situ gas evolution in Li-ion pouch cells. J Electrochem Soc 161(10):A1548–A1554. https://doi.org/10.1149/2.0151410jes
2. An SJ, Li J, Daniel C et al (2016) The state of understanding of the lithium-ion-battery graphite solid electrolyte interphase (SEI) and its relationship to formation cycling. Carbon 105:52–76. https://doi.org/10.1016/j.carbon.2016.04.008
3. Belharouak I, Koenig GM, Tan T et al (2012) Performance degradation and gassing of $Li_4Ti_5O_{12}$/$LiMn_2O_4$ lithium-ion cells. J Electrochem Soc 159(8):A1165–A1170
4. Berg EJ, Villevieille C, Streich D et al (2015) Rechargeable batteries: grasping for the limits of chemistry. J Electrochem Soc 162(14):A2468–A2475
5. Buannic L, Colin JF, Chapuis M et al (2016) Electrochemical performances and gassing behavior of high surface area titanium niobium oxides. J Mater Chem A 4(29):11531–11541. https://doi.org/10.1039/C6TA03813A
6. Cava RJ, Murphy DW, Zahurak SM (1983) Lithium insertion in Wadsley–Roth phases based on niobium oxide. J Electrochem Soc 130(12):2345–2351
7. Colbow KM, Dahn JR, Haering RR (1989) Structure and electrochemistry of the spinel oxides $LiTi_2O_4$ and $Li_{43}Ti_{53}O_4$. J Power Sources 26(3–4):397–402
8. Dean J, Lange N, Forker G et al (1967) Lange's handbook of chemistry. Handbook of chemistry: a reference volume for all requiring ready access to chemical and physical data used in laboratory work and manufacturing. McGraw-Hill, New York
9. Fell CR, Sun L, Hallac PB et al (2015) Investigation of the gas generation in lithium titanate anode based lithium ion batteries. J Electrochem Soc 162(9):A1916–A1920. https://doi.org/10.1149/2.1091509jes
10. Guo B, Yu X, Sun XG et al (2014) A long-life lithium-ion battery with a highly porous $TiNb_2O_7$ anode for large-scale electrical energy storage. Energy Environ Sci 7(7):2220–2226. https://doi.org/10.1039/C4EE00508B
11. Han JT, Goodenough JB (2011) 3-V full cell performance of anode framework $TiNb_2O_7$/spinel $LiNi_{0.5}Mn_{1.5}O_4$. Chem Mater 23(15):3404–3407. https://doi.org/10.1021/cm201515g
12. He YB, Li B, Liu M et al (2012) Gassing in $Li_4Ti_5O_{12}$-based batteries and its remedy. Sci Rep. https://doi.org/10.1038/srep00913
13. He YB, Ning F, Li B et al (2012) Carbon coating to suppress the reduction decomposition of electrolyte on the $Li_4Ti_5O_{12}$ electrode. J Power Sources 202:253–261. https://doi.org/10.1016/j.jpowsour.2011.11.037
14. Hoffmann J, Milien MS, Lucht BL et al (2018) Investigation of gas evolution from $Li_4Ti_5O_{12}$ anode for lithium ion batteries. J Electrochem Soc 165(13):A3108–A3113. https://doi.org/10.1149/2.0741813jes
15. Li H, Zhou H (2012) Enhancing the performances of Li-ion batteries by carbon-coating: present and future. Chem Commun 48(9):1201–1217. https://doi.org/10.1039/C1CC14764A
16. Lv W, Gu J, Niu Y et al (2017) Gassing mechanism and suppressing solutions in Li_{4512}-based lithium-ion batteries. J Electrochem Soc 164(9):A2213–A2224
17. Mercier-Guyon B (2021) Développement d'électrodes négatives à base d'oxydes mixtes de Titane et de Niobium pour accumulateurs Li-ion. PhD thesis, Université Grenoble Alpes
18. Metzger M, Marino C, Sicklinger J et al (2015) Anodic oxidation of conductive carbon and ethylene carbonate in high-voltage Li-ion batteries quantified by on-line electrochemical mass spectrometry. J Electrochem Soc 162(7):A1123–A1134. https://doi.org/10.1149/2.0951506jes
19. Mikolajczak C, Kahn M, White K et al (2012) Lithium-ion batteries hazard and use assessment. Springer, Boston
20. Monroe C, Newman J (2003) Dendrite growth in lithium/polymer systems. J Electrochem Soc 150(10):A1377. https://doi.org/10.1149/1.1606686
21. Parikh D, Geng L, Lyu H et al (2021) Operando analysis of gas evolution in $TiNb_2O_7$ (TNO)-based anodes for advanced high-energy lithium-ion batteries under fast charging. ACS Appl Mater Interfaces 13(46):55145–55155. https://doi.org/10.1021/acsami.1c16866
22. Rowden B, Garcia-Araez N (2020) A review of gas evolution in lithium ion batteries. Energy Rep 6:10–18. https://doi.org/10.1016/j.egyr.2020.02.022
23. Schwenke KU, Solchenbach S, Demeaux J et al (2019) The impact of CO_2 evolved from VC and FEC during formation of graphite anodes in lithium-ion batteries. J Electrochem Soc 166(10):A2035–A2047. https://doi.org/10.1149/2.0821910jes
24. Whittingham S (1976) Electrical energy storage and intercalation chemistry. Science 192(4244):1126–1127. https://doi.org/10.1126/science.192.4244.1126
25. Wu K, Yang J, Zhang Y et al (2012) Investigation on $Li_4Ti_5O_{12}$ batteries developed for hybrid electric vehicle. J Appl Electrochem 42(12):989–995. https://doi.org/10.1007/s10800-012-0442-0
26. Wu K, Yang J, Liu Y et al (2013) Investigation on gas generation of $Li_4Ti_5O_{12}$/$LiNi_{1/3}Co_{1/3}Mn_{1/3}O_2$ cells at elevated temperature. J Power Sources 237:285–290. https://doi.org/10.1016/j.jpowsour.2013.03.057
27. Wu X, Lou S, Cheng X et al (2018) Unravelling the interface layer formation and gas evolution/suppression on a $TiNb_2O_7$ anode for lithium-ion batteries. ACS Appl Mater Interfaces 10(32):27056–27062. https://doi.org/10.1021/acsami.8b08425
28. Yazami R (ed) (2014) Nanomaterials for lithium-ion batteries: fundamentals and applications. Pan Stanford Publications, Singapore
29. Zilio S, Manzi J, Fernicola A et al (2019) Gas release mitigation in LiFePO–$Li_4Ti_5O_{12}$ Li-ion pouch cells by an H_2-selective getter. Electrochim Acta 294:156–165. https://doi.org/10.1016/j.electacta.2018.10.102